

# Dynamics-Guided Diffusion Model for Sensor-less Robot Manipulator Design - *Supplementary Material*

Anonymous Author(s)

Affiliation

Address

email

## 1 Manipulation tasks and metrics

We provide more details about the evaluation manipulation tasks, and introduce more metrics for each task in this section.

Simple objectives:

- **Shift up:** Shift the object upward (along the negative x-axis in the manipulator frame) under all initial poses. For evaluation, we grid sample 360 initial object orientations with positions in the center of the manipulator, and close the manipulator around the object. The average success rate after one closure  $S_x^- \uparrow (\%)$  is reported, where success is counted if the object is shifted more than 3 mm along the negative x-axis. We additionally report continuous metrics including average delta object translation along the x-axis after one closure  $\Delta x \downarrow (\text{cm})$ , and average final x coordinate of the object after the 40th gripper closure  $x \downarrow (\text{cm})$ . The metrics are averaged among the 360 interaction trails with different initial object orientations. The motion objective is  $f(o, m, p) = -\Delta x(o, m, p)$ , then the design objective is aggregated from  $f(o, m, p)$  as  $F(m) = \sum_o \sum_p f(o, m, p)$ .
- **Shift down:** Shift the object downward (along the positive x-axis) under all initial poses. Metrics are average success rate of the object being shifted more than 3 mm along the positive x-axis after one closure  $S_x^+ \uparrow (\%)$ , average delta translation along the x-axis  $\Delta x \uparrow (\text{cm})$ , and average final x coordinate  $x \uparrow (\text{cm})$ . The motion objective is  $f(o, m, p) = \Delta x(o, m, p)$ .
- **Shift left:** Shift the object leftward (along the negative y-axis) under all initial poses. Metrics are average success rate of the object being shifted more than 2 mm along the negative y-axis after one closure  $S_y^- \uparrow (\%)$ , average delta translation along the y-axis  $\Delta y \downarrow (\text{cm})$ , and average final y coordinate  $y \downarrow (\text{cm})$ . The motion objective is  $f(o, m, p) = -\Delta y(o, m, p)$ .
- **Shift right:** Shift the object rightward (along the positive y-axis) under all initial poses. Metrics are average success rate of the object being shifted more than 2 mm along the positive y-axis after one closure  $S_y^+ \uparrow (\%)$ , average delta translation along the y-axis  $\Delta y \uparrow (\text{cm})$ , and average final y coordinate  $y \uparrow (\text{cm})$ . The motion objective is  $f(o, m, p) = \Delta y(o, m, p)$ .
- **Rotate clockwise:** Rotate the object clockwise (negative delta rotation around the z-axis) under all initial poses. Metrics are average success rate of the object being rotated more than 0.03 rad around the negative z-axis after one closure  $S_\theta^- \uparrow (\%)$ , average delta rotation around the z-axis  $\Delta \theta \downarrow (^\circ)$ , and average final orientation  $\theta \downarrow (^\circ)$ . The motion objective is  $f(o, m, p) = -\Delta \theta(o, m, p)$ .
- **Rotate counterclockwise:** Rotate the object counterclockwise (positive delta rotation around the z-axis) under all initial poses. Metrics are average success rate of the object being rotated more than 0.03 rad around the positive z-axis after one closure  $S_\theta^+ \uparrow (\%)$ , average delta rotation around the z-axis  $\Delta \theta \uparrow (^\circ)$ , and average final orientation  $\theta \uparrow (^\circ)$ . The motion objective is  $f(o, m, p) = \Delta \theta(o, m, p)$ .

Complex objectives:

- **Rotate:** Rotate the object either clockwise or counterclockwise under all initial poses. The metrics are average success rate  $S_\theta^{+-} \uparrow (\%)$ , the average absolute value of delta rotation around the z-axis

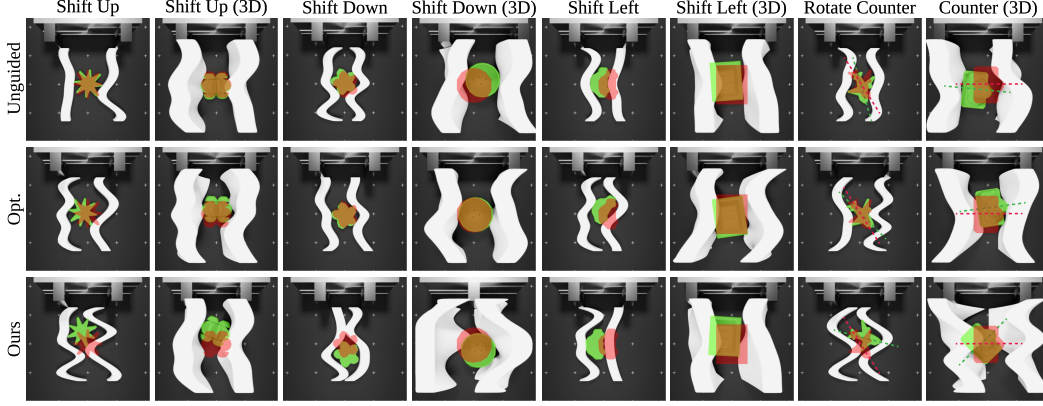


Figure 1: **Results on Simple Objectives.** We generate manipulators for simple objectives that involve motion along one dimension in  $SE_2$  space. Red and green object masks denote object configurations before and after interaction respectively, overlaid with the image after closing in the manipulator. Compared with baseline methods, finger shapes produced by our method achieve the task much more effectively.

- 38  $|\Delta\theta| \downarrow (^{\circ})$ , and the average absolute value of final orientation  $|\theta| \downarrow (^{\circ})$ . The motion objective is  
39  $f(o, m, p) = [\Delta\theta(o, m, p)]^2$ .
- 40 • **Rotate clockwise and shift up:** Rotate the object clockwise and shift it up under all initial  
41 poses. The metrics are average success rate  $S_{\theta}^- \& S_x^- \uparrow (\%)$ , average delta rotation around the  
42 z-axis  $\Delta\theta \downarrow (^{\circ})$ , average final orientation  $\theta \downarrow (^{\circ})$ , average delta translation along the x-axis af-  
43 ter one closure  $\Delta x \downarrow (\text{cm})$ , and average final x coordinate  $x \downarrow (\text{cm})$ . The motion objective is  
44  $f(o, m, p) = -\Delta\theta(o, m, p) - \Delta x(o, m, p)$ .
  - 45 • **Rotate clockwise and shift left:** Rotate the object clockwise and shift it left under all initial  
46 poses. The metrics are average success rate  $S_{\theta}^- \& S_y^- \uparrow (\%)$ , average delta rotation around the z-axis  
47  $\Delta\theta \downarrow (^{\circ})$ , average final orientation  $\theta \downarrow (^{\circ})$ , average delta translation along the y-axis  $\Delta y \downarrow (\text{cm})$ ,  
48 and average final y coordinate  $y \downarrow (\text{cm})$ . The motion objective is  $f(o, m, p) = -\Delta\theta(o, m, p) -$   
49  $\Delta y(o, m, p)$ .
  - 50 • **Convergence:** Reorient the object towards a fixed final pose under a range of initial poses. The  
51 design objective is encouraging the object to rotate in the positive direction when its initial ori-  
52 entation is smaller than the target orientation, or else rotate in the negative direction. The motion  
53 objective is:

$$f(o, m, p) = \begin{cases} \Delta\theta(o, m, p) & \text{if } \theta \in [\theta_{\text{target}} - \pi, \theta_{\text{target}}] \\ -\Delta\theta(o, m, p) & \text{if } \theta \in [\theta_{\text{target}}, \theta_{\text{target}} + \pi] \end{cases} \quad (1)$$

54 To determine the best target orientation  $\theta_{\text{target}}$ , we first forward the dynamics network with the  
55 manipulator shape initialization, object shape, and sampled initial object poses to get a pseudo  
56 interaction profile. We detect the initial object orientation ranges that lead to consecutive positive  
57 delta rotations followed by consecutive negative delta rotations as pseudo convergence ranges.  
58 Then we select the largest pseudo convergence range's corresponding convergence orientation  
59 as  $\theta_{\text{target}}$ . The metric is the maximum convergence range  $R_c^{\text{max}} \uparrow (^{\circ})$ , the largest range of initial  
60 orientations leading to  $\theta_{\text{target}}$  within a small tolerance. We report the maximum convergence range  
61 within the tolerance of  $3^{\circ}$ ,  $5^{\circ}$ , and  $10^{\circ}$ , respectively.

## 62 2 Additional results

63 We report results on all the manipulation tasks and metrics described above in Tab. 1, Tab. 2, Tab. 3,  
64 and Tab. 4. The evaluation procedure is the same as described in the main paper, where we run each  
65 approach 16 times per object-task pair and select the best performance, then average among test  
66 objects. DGDM outperforms baselines consistently on both discrete metrics (e.g. average success  
67 rate) and continuous metrics (e.g. delta object transformation and final transformation).

Table 1: Single Object Simple Objectives Evaluation

		$S_x^- \uparrow$	up $\Delta x \downarrow$	$x \downarrow$	$S_x^+ \uparrow$	down $\Delta x \uparrow$	$x \uparrow$	$S_y^- \uparrow$	left $\Delta y \downarrow$	$y \downarrow$	$S_y^+ \uparrow$	right $\Delta y \uparrow$	$y \uparrow$	$S_\theta^- \uparrow$	clock $\Delta \theta \downarrow$	$\theta \downarrow$	$S_\theta^+ \uparrow$	counter $\Delta \theta \uparrow$	$\theta \uparrow$
2D	Unguided	56.8	-0.2	-1.3	82.1	0.3	1.9	82.9	-0.5	-1.2	80.4	0.5	1.4	46.9	-1.5	-9.5	58.5	2.3	11.1
	Opt.	79.5	-0.4	-2.2	53.3	0.4	2.3	81.3	-0.6	-2.4	94.0	0.7	1.7	48.8	<b>-2.9</b>	-8.8	73.2	3.6	9.6
	DGDM	<b>88.2</b>	<b>-0.4</b>	<b>-3.1</b>	<b>92.0</b>	<b>0.5</b>	<b>3.7</b>	<b>96.7</b>	<b>-0.7</b>	<b>-2.4</b>	<b>97.7</b>	<b>0.8</b>	<b>2.1</b>	<b>60.8</b>	-2.6	<b>-12.3</b>	<b>72.0</b>	<b>3.6</b>	<b>14.2</b>
3D	Unguided	43.0	-0.1	-0.6	43.8	0.1	1.0	80.4	-0.2	-1.2	87.9	0.2	0.9	41.2	-1.1	-4.9	33.5	0.5	2.7
	Opt.	47.4	-0.1	-1.3	66.3	0.2	1.7	86.3	-0.3	-1.3	88.1	0.3	1.6	59.1	-1.9	-5.0	52.0	1.2	4.6
	DGDM	<b>81.5</b>	<b>-0.2</b>	<b>-1.6</b>	<b>75.1</b>	<b>0.2</b>	<b>1.7</b>	<b>95.1</b>	<b>-0.4</b>	<b>-1.8</b>	<b>97.2</b>	<b>0.4</b>	<b>1.9</b>	<b>69.9</b>	<b>-2.3</b>	<b>-7.7</b>	<b>65.0</b>	<b>2.2</b>	<b>6.3</b>

Table 2: Single Object Complex Objectives Evaluation

		$S_\theta^- \uparrow$	rotate $ \Delta \theta  \uparrow$	$ \theta  \uparrow$	$S_\theta^- \& S_x^- \uparrow$	clock-up $\Delta \theta \downarrow$	$\theta \downarrow$	$\Delta x \downarrow$	$x \downarrow$	$S_\theta^- \& S_y^- \uparrow$	clock-left $\Delta \theta \downarrow$	$\theta \downarrow$	$\Delta y \downarrow$	$y \downarrow$	$R_c^{max}(3^\circ) \uparrow$	convergence $R_c^{max}(5^\circ) \uparrow$	$R_c^{max}(10^\circ) \uparrow$
2D	Unguided	74.0	3.5	18.2	36.4	-1.5	-9.5	-0.2	-1.3	36.9	-1.5	-9.5	-0.5	-1.2	56.5	61.7	68.7
	Opt.	78.9	4.5	18.9	29.3	-1.8	-4.2	-0.3	-1.0	49.4	-2.9	-9.0	-0.6	-2.1	69.6	73.7	82.1
	DGDM	<b>79.3</b>	<b>4.5</b>	<b>20.1</b>	<b>62.7</b>	<b>-3.3</b>	<b>-14.5</b>	<b>-0.4</b>	<b>-3.6</b>	<b>63.7</b>	<b>-3.2</b>	<b>-10.1</b>	<b>-0.7</b>	<b>-2.4</b>	<b>78.4</b>	<b>83</b>	<b>89.3</b>
3D	Unguided	64.2	2.2	16.5	30.3	-1.1	-4.9	-0.1	-0.6	33.1	-0.5	-2.7	-0.2	-1.2	52.2	63.6	67.8
	Opt.	66.9	2.4	15.7	29.2	-1.1	-2.7	-0.1	-0.5	37.7	-1.3	-3.3	-0.3	-1.0	50.3	60	72.3
	DGDM	<b>83.0</b>	<b>3.1</b>	<b>21.0</b>	<b>57.1</b>	<b>-2.4</b>	<b>-6.8</b>	<b>-0.2</b>	<b>-0.9</b>	<b>58.2</b>	<b>-2.9</b>	<b>-11.1</b>	<b>-0.5</b>	<b>-1.7</b>	<b>68.8</b>	<b>72.5</b>	<b>81.5</b>

Table 3: Multi-object Simple Objectives Evaluation

		$S_x^- \uparrow$	up $\Delta x \downarrow$	$x \downarrow$	$S_x^+ \uparrow$	down $\Delta x \uparrow$	$x \uparrow$	$S_y^- \uparrow$	left $\Delta y \downarrow$	$y \downarrow$	$S_y^+ \uparrow$	right $\Delta y \uparrow$	$y \uparrow$	$S_\theta^- \uparrow$	clock $\Delta \theta \downarrow$	$\theta \downarrow$	$S_\theta^+ \uparrow$	counter $\Delta \theta \uparrow$	$\theta \uparrow$
2D	Unguided	55.8	-0.2	-1.3	79.8	0.3	1.3	77.1	-0.5	-1.1	80.3	0.5	1.3	44.7	-1.5	-3.5	56.4	2.1	6.2
	Opt.	78.6	-0.4	-1.0	50.3	0.3	1.0	79.2	-0.6	-1.0	93.8	0.7	1.7	46.1	<b>-2.9</b>	-7.8	71.4	<b>3.5</b>	7.4
	DGDM	<b>83.8</b>	<b>-0.4</b>	<b>-3.0</b>	<b>88.1</b>	<b>0.4</b>	<b>3.4</b>	<b>99.3</b>	<b>-0.7</b>	<b>-2.5</b>	<b>94.3</b>	<b>0.7</b>	<b>2.1</b>	<b>61.3</b>	-2.4	<b>-10.5</b>	<b>68.4</b>	3.3	<b>16.5</b>
3D	Unguided	40.1	-0.1	-0.5	40.8	0.1	0.9	75.8	-0.2	-0.8	87.9	0.2	0.6	34.7	-0.5	-0.8	29.2	0.1	2.5
	Opt.	42.4	-0.1	-0.4	66.4	0.2	1.0	77.9	-0.2	-0.4	86.6	0.3	0.8	40.3	-1.1	-1.9	39.2	<b>1.9</b>	3.5
	DGDM	<b>89.7</b>	<b>-0.2</b>	<b>-1.5</b>	<b>66.8</b>	<b>0.2</b>	<b>1.2</b>	<b>96.1</b>	<b>-0.5</b>	<b>-1.8</b>	<b>95.4</b>	<b>0.4</b>	<b>1.3</b>	<b>69.3</b>	<b>-2.0</b>	<b>-5.2</b>	<b>58.2</b>	1.6	<b>3.5</b>

Table 4: Multi-object Complex Objectives Evaluation

		$S_\theta^- \uparrow$	rotate $ \Delta \theta  \uparrow$	$ \theta  \uparrow$	$S_\theta^- \& S_x^- \uparrow$	clock-up $\Delta \theta \downarrow$	$\theta \downarrow$	$\Delta x \downarrow$	$x \downarrow$	$S_\theta^- \& S_y^- \uparrow$	clock-left $\Delta \theta \downarrow$	$\theta \downarrow$	$\Delta y \downarrow$	$y \downarrow$
2D	Unguided	68.3	3.2	13.4	35.2	-1.5	-3.5	-0.2	-0.8	35.2	-1.0	-3.0	-0.5	-1.0
	Opt.	74.3	3.8	7.2	25.0	-1.4	-0.1	-0.1	-0.2	49.0	-2.9	-4.6	-0.4	-0.7
	DGDM	<b>78.4</b>	<b>4.2</b>	<b>15.8</b>	<b>62.4</b>	<b>-3.3</b>	<b>-10.6</b>	<b>-0.4</b>	<b>-3.6</b>	<b>63.8</b>	<b>-3.0</b>	<b>-6.3</b>	<b>-0.7</b>	<b>-2.4</b>
3D	Unguided	61.7	2.1	15.8	29.2	-0.8	-0.4	-0.1	-0.5	25.2	0.1	2.5	-0.2	-0.7
	Opt.	67.0	2.3	9.5	22.6	0.1	-0.1	-0.1	-0.3	34.3	-0.9	-1.2	-0.2	-0.5
	DGDM	<b>77.6</b>	<b>2.5</b>	<b>21.6</b>	<b>44.2</b>	<b>-1.6</b>	<b>-7.6</b>	<b>-0.2</b>	<b>-1.2</b>	<b>37.9</b>	<b>-2.3</b>	<b>-8.9</b>	<b>-0.5</b>	<b>-2.3</b>

### 68 3 Discussions

69 **Modeling Interactions instead of Modeling Contacts.** Differentiable simulator [1, 2, 3, 4, 5] is an-  
70 other popular choice for providing the gradient of design objective  $\nabla_m F$ , but suffers from two major  
71 limitations. First, soft contact models, such as penalty-based methods used by Xu et al., are known  
72 to yield biased and high-variance gradients [6, 2]. Further, such gradients need to be computed for  
73 each simulation timestep, which is computationally expensive for long-horizon interactions. Instead  
74 of modeling individual contacts, our dynamics network learns to capture the temporally extended  
75 finger-object interaction. It is trained on physically accurate simulated data, avoiding the limitations  
76 associated with soft contacts. Moreover, our dynamics network generalizes to novel objects and  
77 tasks at test time, allowing for constructing new objectives without extra data generation or training.

## References

- [1] J. Xu, T. Chen, L. Zlokapa, M. Foshey, W. Matusik, S. Sueda, and P. Agrawal. [An End-to-End Differentiable Framework for Contact-Aware Robot Design](#). In *Robotics: Science & Systems*, 2021.
- [2] M. Li, R. Antonova, D. Sadigh, and J. Bohg. [Learning tool morphology for contact-rich manipulation tasks with differentiable simulation](#). In *2023 IEEE International Conference on Robotics and Automation (ICRA)*, pages 1859–1865. IEEE, 2023.
- [3] T.-H. J. Wang, J. Zheng, P. Ma, Y. Du, B. Kim, A. Spielberg, J. Tenenbaum, C. Gan, and D. Rus. [DiffuseBot: Breeding Soft Robots With Physics-Augmented Generative Diffusion Models](#). *Advances in Neural Information Processing Systems*, 36, 2024.
- [4] A. Spielberg, A. Zhao, Y. Hu, T. Du, W. Matusik, and D. Rus. [Learning-in-the-loop optimization: End-to-end control and co-design of soft robots through learned deep latent representations](#). *Advances in Neural Information Processing Systems*, 32, 2019.
- [5] Y. Hu, J. Liu, A. Spielberg, J. B. Tenenbaum, W. T. Freeman, J. Wu, D. Rus, and W. Matusik. [Chainqueen: A real-time differentiable physical simulator for soft robotics](#). In *2019 International conference on robotics and automation (ICRA)*, pages 6265–6271. IEEE, 2019.
- [6] H. T. Suh, M. Simchowitz, K. Zhang, T. Pang, and R. Tedrake. [Pathologies and Challenges of Using Differentiable Simulators in Policy Optimization for Contact-Rich Manipulation](#). In *ICRA 2022 Workshop: Reinforcement Learning for Contact-Rich Manipulation*, 2022.